

# STRUCTURE OF ICOSAHEDRAL BORIDES BY RAMAN SPECTROSCOPY\*

SAND--91-0236C

D. R. Tallant, T. L. Aselage, and D. Emin  
Sandia National Laboratories  
Albuquerque, NM 87185

DE91 010872

## ABSTRACT

We have obtained Raman spectra of icosahedral boron-rich solids. The spectra of  $\alpha$ -rhombohedral boron, boron arsenide, and boron phosphide are consistent with highly ordered materials. Polarization studies have resulted in symmetry assignments for most of the Raman bands of  $\alpha$ -rhombohedral boron. In contrast, the Raman spectra of the boron carbides reveal local substitutional disorder. They also change progressively as a function of carbon content. A structural model for the boron carbides has been developed to explain the Raman and infrared absorption spectra, x-ray data, and electrical and thermal transport properties. Raman spectra of boron carbide samples enriched in  $^{10}\text{B}$ ,  $^{11}\text{B}$ , and  $^{13}\text{C}$  reveal details of the atomic motions. The vibrational frequencies and exceptionally narrow linewidths of certain Raman modes are discussed in terms of a "strong" bond model. In this model certain vibrational modes involving relatively stiff bonds between chain atoms, chain and icosahedral atoms, and atoms on different icosahedra are decoupled from the boride lattice by weak, intraicosahedral bonds.

## INTRODUCTION

Icosahedral boron-rich solids are refractory materials with high melting points.

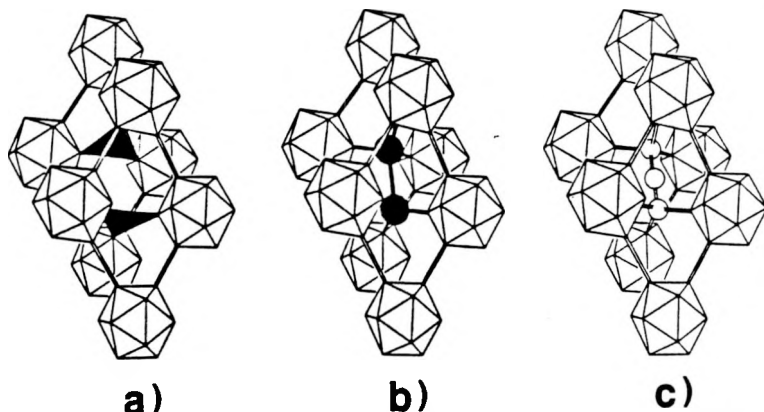


Fig. 1. Icosahedral borides. (a)  $\alpha$ -rhombohedral boron, (b) boron phosphide or boron arsenide, (c) boron carbide.

melting temperatures up to 2400°C. Their structures are based on the structure of  $\alpha$ -rhombohedral boron.<sup>1</sup> As illustrated in Figure 1a,  $\alpha$ -rhombohedral boron is composed of boron icosahedra (twelve-atom clusters) located at the corners of a rhombohedral unit cell.<sup>2</sup> Three-

\*This work was performed at Sandia National Laboratories supported by Office of Basic Energy Sciences, Division of Materials Sciences, U.S. Dept. of Energy under Contract Number DE-AC04-76-DP00789.

DISTRIBUTION OF THIS DOCUMENT IS UNLIMITED

# MASTER

## **DISCLAIMER**

**This report was prepared as an account of work sponsored by an agency of the United States Government. Neither the United States Government nor any agency thereof, nor any of their employees, makes any warranty, express or implied, or assumes any legal liability or responsibility for the accuracy, completeness, or usefulness of any information, apparatus, product, or process disclosed, or represents that its use would not infringe privately owned rights. Reference herein to any specific commercial product, process, or service by trade name, trademark, manufacturer, or otherwise does not necessarily constitute or imply its endorsement, recommendation, or favoring by the United States Government or any agency thereof. The views and opinions of authors expressed herein do not necessarily state or reflect those of the United States Government or any agency thereof.**

---

## **DISCLAIMER**

**Portions of this document may be illegible in electronic image products. Images are produced from the best available original document.**

## **DISCLAIMER**

This report was prepared as an account of work sponsored by an agency of the United States Government. Neither the United States Government nor any agency thereof, nor any of their employees, makes any warranty, express or implied, or assumes any legal liability or responsibility for the accuracy, completeness, or usefulness of any information, apparatus, product, or process disclosed, or represents that its use would not infringe privately owned rights. Reference herein to any specific commercial product, process, or service by trade name, trademark, manufacturer, or otherwise does not necessarily constitute or imply its endorsement, recommendation, or favoring by the United States Government or any agency thereof. The views and opinions of authors expressed herein do not necessarily state or reflect those of the United States Government or any agency thereof.

center bonds (the shaded triangles in Figure 1a) join icosahedra along the three-fold axis of the unit cell. In the icosahedral boron-rich pnictides ( $B_{12}P_2$  or  $B_{12}As_2$ , Figure 1b), a chain composed of two phosphorus or two arsenic atoms joins the icosahedra. In the boron carbides (Figure 1c), a three-atom chain joins the icosahedra. Both types of chain structures reside along the longest diagonal of the unit cell. In each icosahedron of all three types of boron-rich solids, six atoms bond directly to other icosahedra via stiff two-center bonds along the cell edges. These six atoms reside in two "polar" triangles on opposite ends of the icosahedron. The remaining six icosahedral atoms, occupying "equatorial" sites, either bond directly to other icosahedra through three-center bonds, as in  $\alpha$ -rhombohedral boron, or bond to chain structures, as in the boron pnictides and carbides.

The boron-rich pnictides, when present in a well-defined stoichiometry ( $B_{12}P_2$  or  $B_{12}As_2$ ) are wide-band-gap insulators. If suitably doped, they may have applications as high temperature semiconductors.<sup>3</sup> The boron carbides exist as a single-phase material from ~9 at.% carbon to ~20 at.% carbon.<sup>4</sup> They are degenerate, p-type semiconductors with potential applications as high temperature thermoelectric materials.<sup>5</sup> X-ray<sup>1</sup> and electrical and thermal transport measurements (summarized in Ref. 6) suggest that, at 20 at.% carbon, boron carbides are composed of  $B_{11}C$  icosahedra and carbon-boron-carbon (CBC) chains. With decreasing carbon content, CBC chains are progressively replaced by CBB chains.

This paper describes the results of Raman studies on  $\alpha$ -rhombohedral boron, the boron pnictides, and the boron carbides. This work includes a polarization study of  $\alpha$ -rhombohedral boron. Raman studies were carried out on the boron carbides both as a function of carbon concentration and as a function of isotopic ( $^{10}B$ ,  $^{11}B$ , and  $^{13}C$ ) enrichment. The exceptionally narrow bandwidths of certain Raman bands are explained by the decoupling of their vibrational modes from the boride lattice. Decoupling occurs when bonds internal to the groups of atoms involved in the vibrational motion are much stiffer than those by which they are attached to the remainder of the lattice.

## EXPERIMENTAL

Polycrystalline boron carbide samples, including those isotopically enriched, were prepared by hot pressing of boron carbide powders or mixtures of boron and graphite powders. Single crystals of  $\alpha$ -rhombohedral boron, icosahedral boron arsenide, and boron carbide were prepared by recrystallization from molten copper- and palladium-boron alloys. The icosahedral boron phosphide ( $B_{12}P_2$ ) sample was obtained in powder form from Noah Chemical Company.

Raman spectra were obtained using a computer-controlled, scanning double monochromator equipped with holographic gratings and a photon-counting photomultiplier tube. The 514.5nm argon ion laser line was used for excitation. Additional experimental details have been provided elsewhere.<sup>6</sup>

### BORIDE RAMAN SPECTRA

Figure 2 displays the Raman spectra of (from top to bottom) a single crystal of boron arsenide, boron phosphide powder, a single

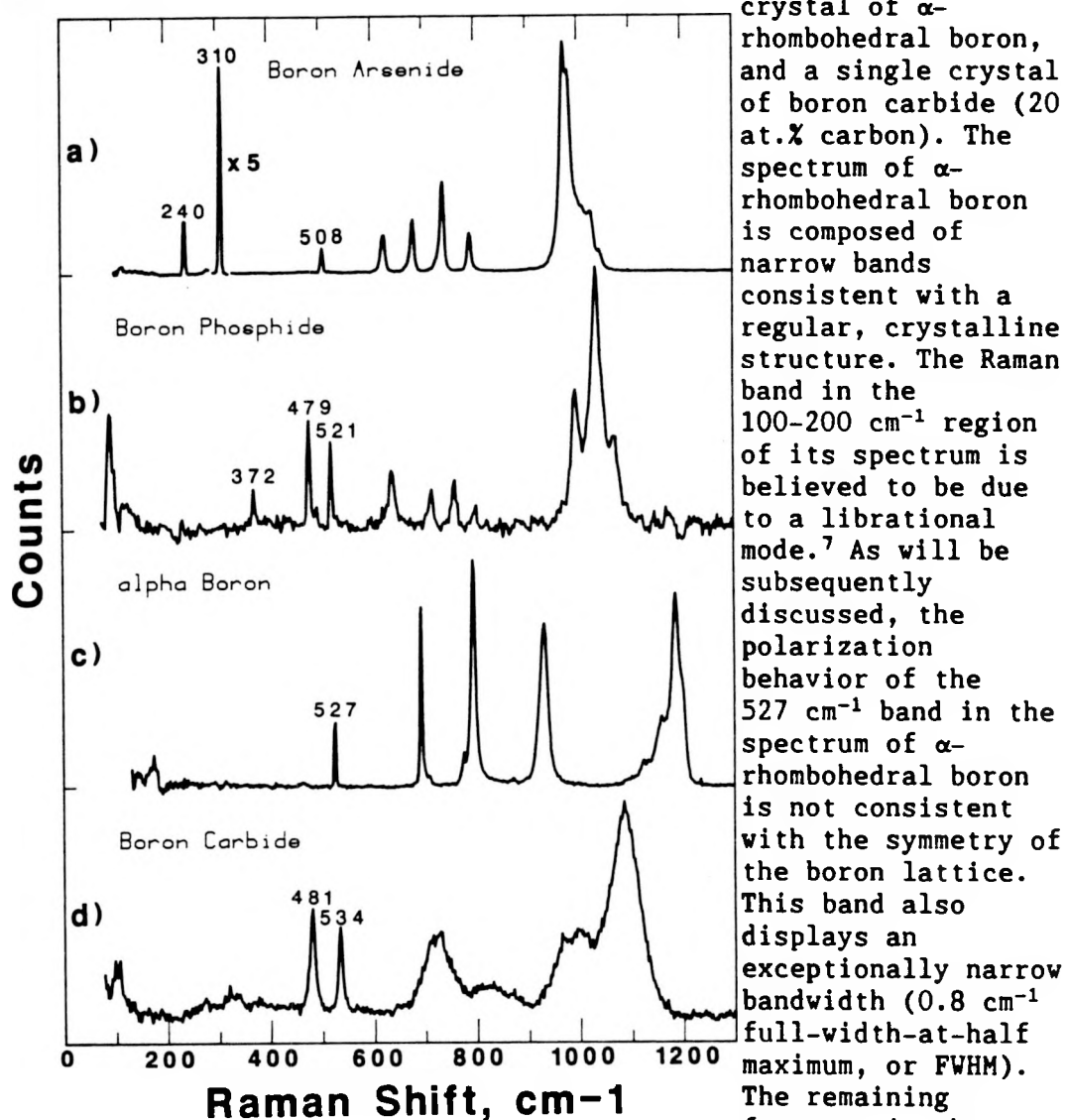


Fig. 2. Raman spectra of icosahedral borides. (a) Single-crystal boron arsenide, (b) boron phosphide powder, (c) single-crystal  $\alpha$ -rhombohedral boron, (d) single-crystal boron carbide (20 at.% carbon).

crystal of  $\alpha$ -rhombohedral boron, and a single crystal of boron carbide (20 at.% carbon). The spectrum of  $\alpha$ -rhombohedral boron is composed of narrow bands consistent with a regular, crystalline structure. The Raman band in the 100-200  $\text{cm}^{-1}$  region of its spectrum is believed to be due to a librational mode.<sup>7</sup> As will be subsequently discussed, the polarization behavior of the 527  $\text{cm}^{-1}$  band in the spectrum of  $\alpha$ -rhombohedral boron is not consistent with the symmetry of the boron lattice. This band also displays an exceptionally narrow bandwidth (0.8  $\text{cm}^{-1}$  full-width-at-half maximum, or FWHM). The remaining features in the spectrum of  $\alpha$ -rhombohedral boron range in frequency from 690 to 1200  $\text{cm}^{-1}$ . These

features have been assigned to vibrational motions of intraicosahedral or intericosahedral boron-boron bands.<sup>6</sup> Note that the band complex at 1100 to 1200  $\text{cm}^{-1}$ , which has been associated with an icosahedral breathing mode<sup>8</sup>, represents the overlap of a number of narrow bands. Changing the orientation of the crystal makes the contributions of the individual bands more apparent.

The Raman bands in the spectra of the two icosahedral boron pnictides (Figures 2a and 2b) also have the narrow bandwidths characteristic of ordered materials. As with  $\alpha$ -rhombohedral boron, the higher frequency bands (600 to 1100  $\text{cm}^{-1}$ ), are assigned to intraicosahedral or intericosahedral vibrational modes. Bands at 508  $\text{cm}^{-1}$  (boron arsenide) and 518  $\text{cm}^{-1}$  (boron phosphide) may have an origin similar to that of the 527  $\text{cm}^{-1}$  band (see following section) in the  $\alpha$ -rhombohedral boron spectrum. Unlike the spectrum of  $\alpha$ -rhombohedral boron, the Raman spectra of the icosahedral boron pnictides have low-frequency features. The 310  $\text{cm}^{-1}$  band in the boron arsenide spectrum and the 472  $\text{cm}^{-1}$  band in the boron phosphide spectrum have been assigned, respectively, to As-As and P-P stretching modes.<sup>6</sup> The 240  $\text{cm}^{-1}$  band in the boron arsenide spectrum and the 369  $\text{cm}^{-1}$  band in the boron phosphide spectrum may be due to chain-icosahedron (B-As or B-P) modes.

In contrast to the  $\alpha$ -rhombohedral boron and boron pnictide spectra of Figure 2 (a,b, and c), the Raman spectrum of boron carbide with 20 at.% carbon (Figure 2d) displays relatively broad bands in the region above 600  $\text{cm}^{-1}$ . This frequency region is characteristic of intraicosahedral or intericosahedral vibrational modes. The breadth of these bands is the result of a kind of substitutional disorder. This substitutional disorder results from the presence of a carbon atom residing in any one of six polar positions in primarily boron icosahedra.<sup>6</sup> Thus, the high frequency region of the boron carbide spectrum indicates the presence of  $\text{B}_{11}\text{C}$  icosahedra.

The 481 and 534  $\text{cm}^{-1}$  bands in the boron carbide spectrum are relatively narrow, suggesting an origin in a more ordered environment than the icosahedra. Because of the dependence of their intensity on the carbon content (this effect will be discussed in a later section), these bands cannot have the same origin as the 527  $\text{cm}^{-1}$  band of  $\alpha$ -rhombohedral boron. The frequencies, isotopic dependences, and bandwidths of these bands are consistent, however, with carbon-containing intericosahedral chain structures that exist in a relatively ordered environment.<sup>6</sup> A boron carbide structure consisting of  $\text{B}_{11}\text{C}$  icosahedra linked by CBC chains corresponds to a carbon content of 20 at.% and is consistent with the electrical and thermal transport properties of this composition.

#### POLARIZATION STUDY OF $\alpha$ -RHOBOHEDRAL BORON

Using the microscope attachment of the Raman spectrometer, a polarization study was carried out on an oriented crystal of

$\alpha$ -rhombohedral boron. The  $D_{3d}$  point group of  $\alpha$ -rhombohedral boron allows Raman activity for modes of  $A_{1g}$  and  $E_g$  symmetry.<sup>9</sup> In Porto notation<sup>10</sup>, the combination of crystal and polarization analyzer orientations designated Y(ZZ)Y should yield only bands of  $A_{1g}$  symmetry. The orientations designated Y(ZX)Y should yield only bands of  $E_g$  symmetry. Spectra of  $\alpha$ -rhombohedral boron obtained with these symmetries are shown in Figure 3. The large numerical aperture of the microscope objective used to focus the laser source onto the crystal of  $\alpha$ -rhombohedral boron allowed some mixing of symmetries in the two orientations, but the trends are clear. The most intense bands in the spectrum of  $\alpha$ -rhombohedral boron obtained without polarization analysis (Figure 2c) all show  $A_{1g}$  symmetry character. Only two weak bands near 750 and 1100  $\text{cm}^{-1}$  show evidence of  $E_g$  symmetry character. The 527  $\text{cm}^{-1}$  band shows approximately the same intensity in both the Y(ZZ)Y and Y(ZX)Y orientations. None of the symmetry groups that are Raman-active in the  $D_{3d}$  point group should display this behavior. As noted previously, the Raman band at 527  $\text{cm}^{-1}$  has an exceptionally narrow bandwidth (0.8  $\text{cm}^{-1}$  FWHM). This bandwidth is approximately an order of magnitude smaller than those of the rest of the  $\alpha$ -rhombohedral boron Raman bands. The 527  $\text{cm}^{-1}$  band appears to be due to an inelastic scattering phenomenon, since it occurs at the same frequency in spectra obtained with different laser excitation wavelengths. However, the exceptionally narrow bandwidth and the unusual polarization behavior of the 527  $\text{cm}^{-1}$  band distinguish it from the other Raman

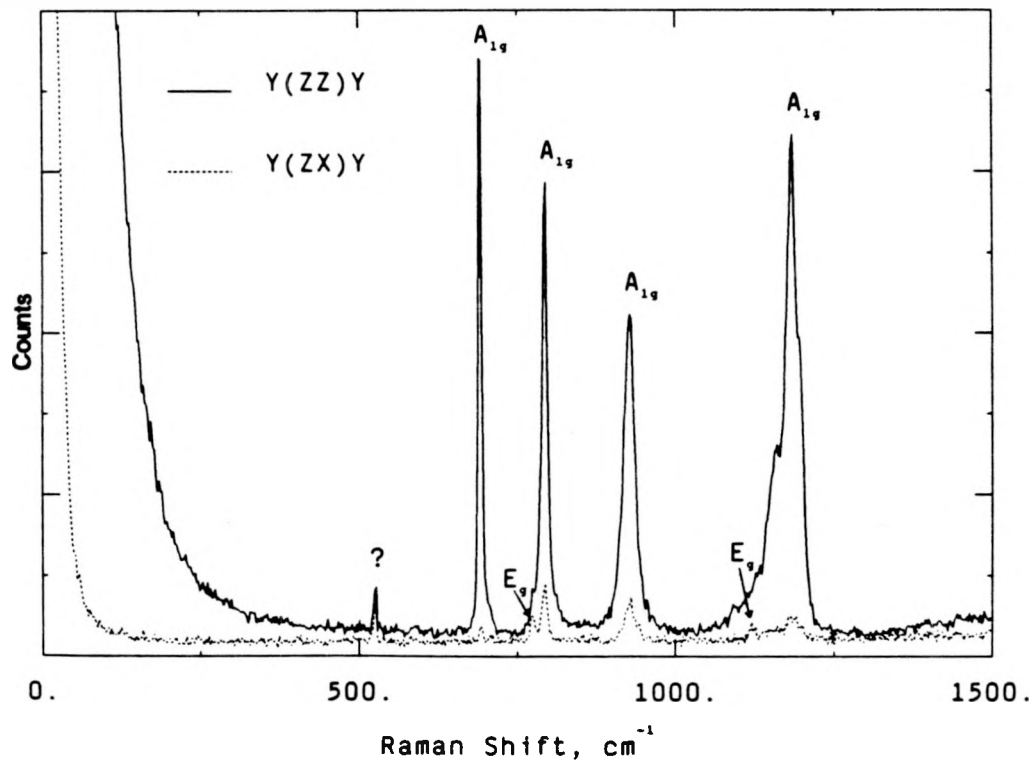


Fig. 3. Raman spectra of a single crystal of  $\alpha$ -rhombohedral boron in Y(ZZ)Y and Y(ZX)Y orientations (Porto notation).

bands of  $\alpha$ -rhombohedral boron which behave like local vibrational modes. Investigations to determine the source of this feature are continuing.

#### BORON CARBIDES - COMPOSITION DEPENDENCE

Figure 4 displays Raman spectra of a set of isotopically-enriched ( $^{11}\text{B}$ ) boron carbides ranging from 20 to 10 at.% carbon. The bands above  $600\text{ cm}^{-1}$ , associated with icosahedral vibrational modes, show only minor changes as a function of carbon content over this concentration range. As previously noted, the icosahedra have the  $\text{B}_{11}\text{C}$  composition at 20 at.% carbon. Apparently, most of the icosahedra retain this composition even as the carbon content of

the matrix is halved. On the other hand, the narrow bands at 481 and  $534\text{ cm}^{-1}$ , associated with chain vibrational modes, disappear and are replaced by broader bands near  $400\text{ cm}^{-1}$  as the carbon content decreases. These changes in the Raman spectra with decreasing carbon content are consistent with the replacement of CBC chains by CBB chains. CBB chains are less stiff<sup>11</sup> and have lower vibrational frequencies than the CBC chains they replace. The bands due to CBB chain modes are relatively broad because the boron end of the chain can bond to either a boron or a carbon in an equatorial position on a neighboring icosahedron, whereas carbon chain terminators bond exclusively to

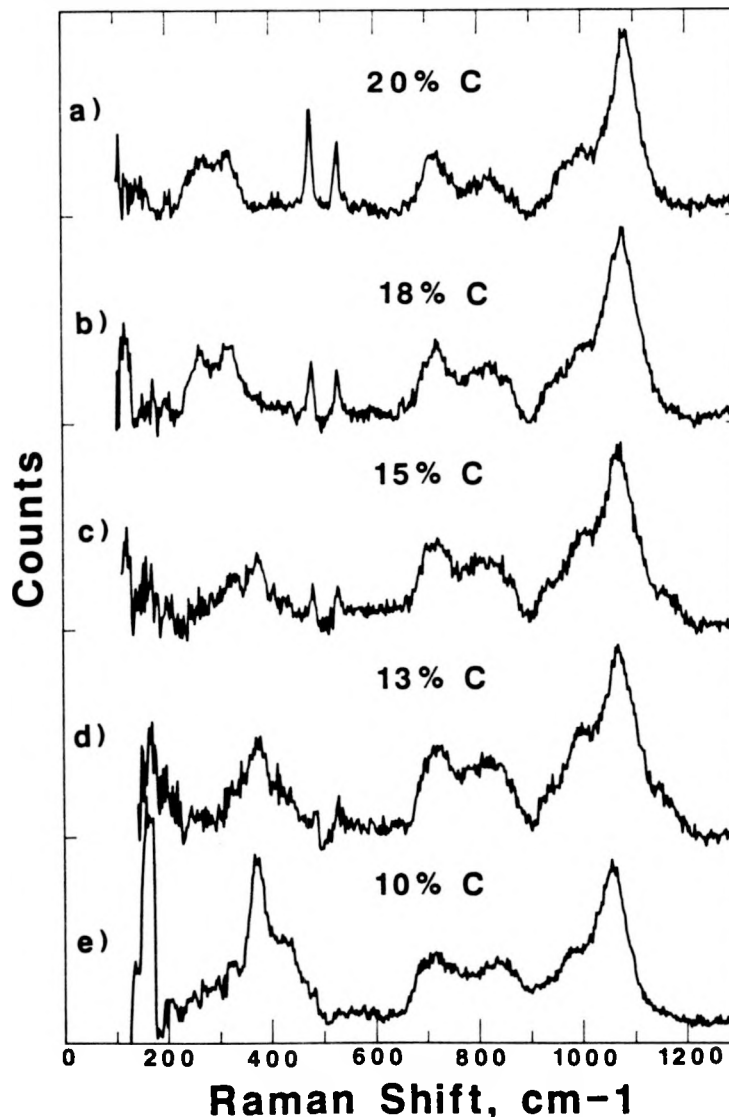


Fig. 4. Raman spectra of hot-pressed, isotopically enriched ( $^{11}\text{B}$ ) boron carbides. Compositions in atomic % carbon.

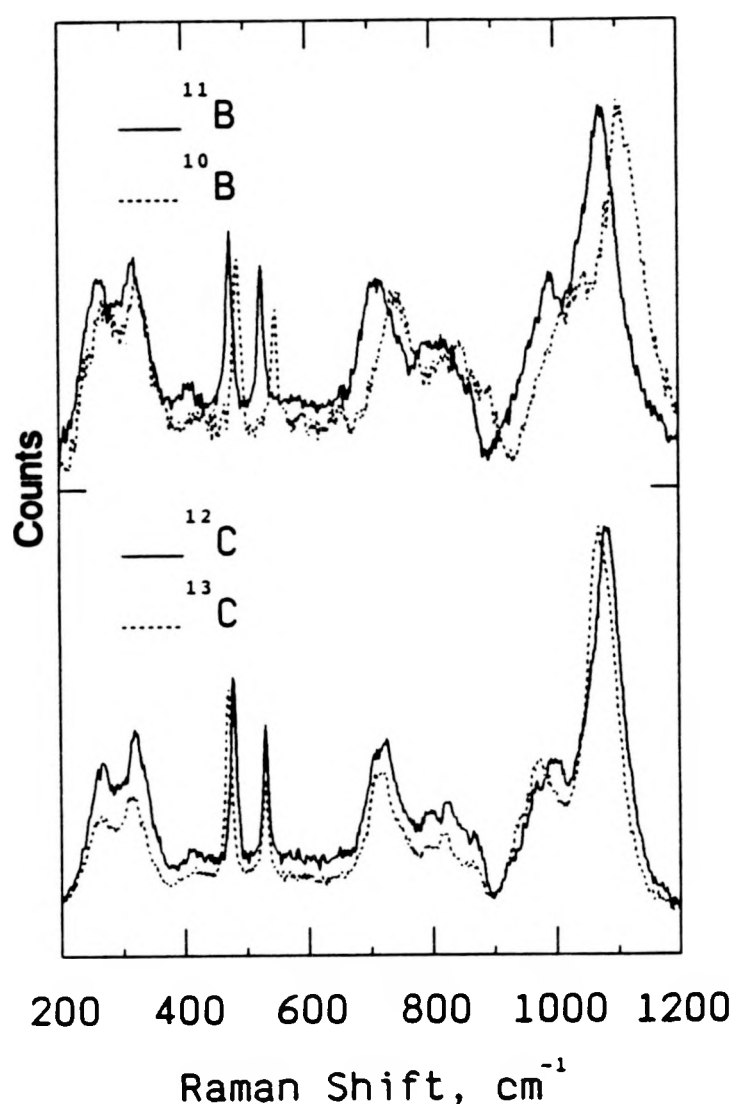


Fig. 5. Raman spectra of boron carbide with 20 at.% carbon and isotopic enrichments as shown in the figure.

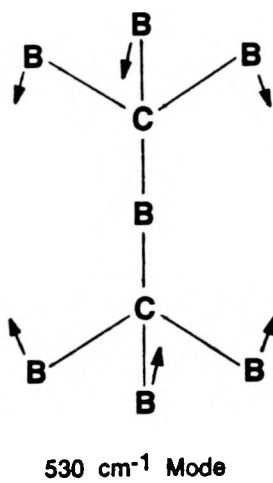
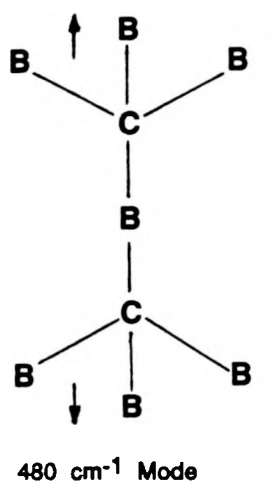
in the  $B_{11}C$  icosahedra) as the carbon content decreases from 20 at.%, then at 13 at.% carbon all the CBC chains will have been replaced by CBB chains. Reductions in the carbon content below 13 at.% are expected to result in the replacement of  $B_{11}C$  icosahedra by  $B_{12}$  icosahedra.<sup>12</sup> Raman spectroscopic data supports this expectation.<sup>6</sup> Thus, Raman, x-ray, and electrical and thermal transport data are consistent with the following model for boron carbide. At 20 at.% carbon, boron carbide consists of  $B_{11}C$  icosahedra and CBC chains. From 20 to 13 at.% carbon, CBC chains are replaced by CBB chains. Below 13 at.% carbon,  $B_{11}C$  icosahedra are replaced by  $B_{12}$  icosahedra.

icosahedral borons<sup>6</sup>. Differences in orientation of CBB chains combined with variation in their chain-icosahedral bonding "disorder" the local environment and cause broadening of the associated vibrational bands. A consequence of the appearance of CBB chains is the presence of carbon atoms in equatorial positions, as well as polar positions, of the  $B_{11}C$  icosahedra. The net result is an increase in substitutional disorder in the icosahedra, which is observed as a slight broadening of some Raman bands associated with icosahedral modes (compare the band peaking near  $1100\text{ cm}^{-1}$  for the 20 and 13 at.% carbon samples in Figure 4). If boron replaces carbon only in the chains (not

## BORON CARBIDES - ISOTOPIC SUBSTITUTION

Raman spectra were obtained of boron carbide samples containing 20 and 10 at.% carbon and separately enriched in  $^{10}\text{B}$ ,  $^{11}\text{B}$ , and  $^{13}\text{C}$ . Raman spectra were also obtained of a boron carbide sample containing 13 at.% carbon enriched in  $^{13}\text{C}$ . All of the Raman bands in the samples containing 10 and 20 at.% carbon showed boron isotope shifts, indicating that significant boron motion is involved in all the Raman-active vibrational modes. The Raman band between 1000 and 1100  $\text{cm}^{-1}$  in the samples containing 10, 13, and 20 at.% carbon also showed a carbon isotope shift. Since this Raman band is due to a pure icosahedral vibrational mode<sup>6</sup>, a carbon isotope shift indicates that carbon atoms are present in icosahedra not only at the higher carbon contents but even at 10 at.% carbon. This result confirms that some  $\text{B}_{11}\text{C}$  icosahedra persist to low carbon concentrations, as predicted by the model derived from Raman, x-ray, and electrical and thermal transport data.

Raman spectra of isotopically-substituted boron carbide with 20 atomic % carbon are presented in Figure 5. Two sets of samples were examined: one set of two samples with naturally-occurring carbon isotopes and  $^{10}\text{B}$  and  $^{11}\text{B}$  enrichment; and one set of two samples enriched in  $^{11}\text{B}$  and with naturally-occurring carbon and  $^{13}\text{C}$ . Spectra of the samples in each set were obtained immediately after each other to minimize the effects of instrumental drift. Frequencies for a set of samples are reproducible to less than 2  $\text{cm}^{-1}$ . The narrow Raman bands associated with CBC chain modes and occurring near 480 and 530  $\text{cm}^{-1}$  display the isotopic shifts shown in Table I.



These isotope shifts are consistent with the atomic motions shown in Figure 6. The lower frequency chain mode is an in-phase stretching motion of  $\text{CB}_3$  groups (carbon stiffly bonded to three icosahedral borons in equatorial positions) about the boron in the center of the chain. The higher frequency mode involves almost exclusively boron

Fig. 6. Vibrational modes of boron carbide (20 at.% C) involving chain atoms.

motion with the icosahedral boron atoms bending umbrella-like about a chain carbon. These modes appear as narrow ( $\sim 5 \text{ cm}^{-1}$  FWHM) Raman bands because their local environment is relatively ordered compared to the icosahedra. As will be discussed in the next section, the relatively stiff chain-carbon-to-icosahedral-boron

bonds are largely decoupled from rest of the boron carbide matrix by weak intraicosahedral and weak chain carbon-chain boron bonds.

TABLE I  
ISOTOPIC SHIFTS  
(Boron Carbide, 20 at.% C, CBC chain modes)

Isotopes	481 $\text{cm}^{-1}$ Band	534 $\text{cm}^{-1}$ Band
$^{10}\text{B}/^{11}\text{B}$	12 $\text{cm}^{-1}$	23 $\text{cm}^{-1}$
$^{12}\text{C}/^{13}\text{C}$	7 $\text{cm}^{-1}$	1 $\text{cm}^{-1}$

#### THE "STRONG BOND" MODEL

The frequencies and exceptionally narrow widths of certain Raman bands of the icosahedral borides can be explained by the disparity between the strengths of different types of boride bonds. Emin<sup>13</sup> has recognized that the intraicosahedral bonds outside of the polar triangle are weak compared to the intericosahedral and chain-icosahedral bonds. From a classical treatment of Raman bandwidths, Laulicht and Halpern<sup>14</sup> determined that a primary broadening mechanism of a Raman vibrational mode is the damping of the vibrational motion by bonds to atoms not directly involved in the vibrational mode. Thus, if the atoms of a vibrational mode are largely decoupled from neighboring atoms by relatively weak bonds, and if the local environment of the mode is highly ordered, the mode should display a very narrow bandwidth.

Exceptionally narrow ( $<1 \text{ cm}^{-1}$ ) Raman bandwidths occur not only, as has been noted, for the  $527 \text{ cm}^{-1}$  band of  $\alpha$ -rhombohedral boron but also for the 240, 310, and  $508 \text{ cm}^{-1}$  bands of boron arsenide (Figure 2).

Of these Raman bands, the origin of only the  $310 \text{ cm}^{-1}$  band of boron arsenide is known with certainty. The vibrational mode related to this Raman band is the in-phase stretching motion of two  $\text{AsB}_3$  groups against each other<sup>6</sup> (Figure 7). The boron atoms in the  $\text{AsB}_3$  groups reside in equatorial positions on different  $\text{B}_{12}$

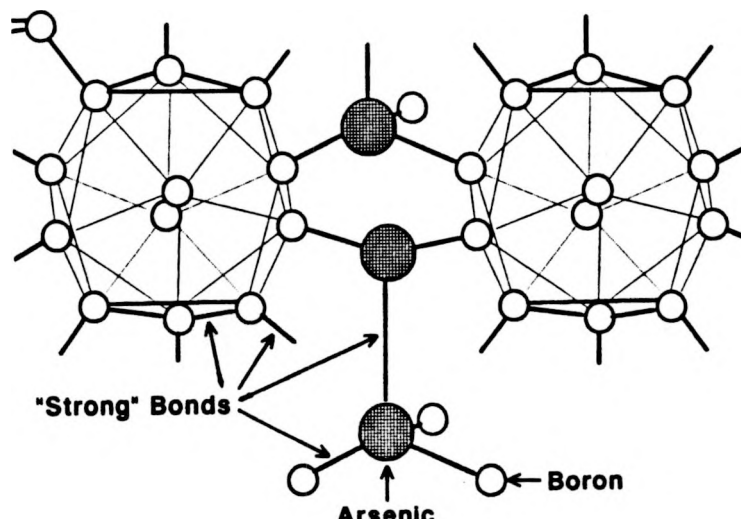
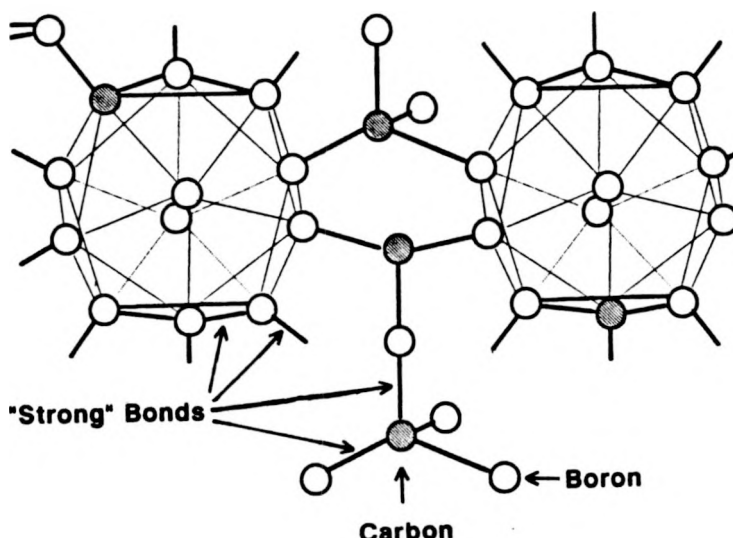


Fig. 7. Boron arsenide ( $\text{B}_{12}\text{As}_2$ ) structure.



icosahedra. The width of the  $310\text{ cm}^{-1}$  band, when deconvoluted from the instrumental line function, is  $0.43\text{ cm}^{-1}$ . Stiff ("strong") As-As and As-B bonds are decoupled from other stiff bonds by relatively weak intraicosahedral bonds, resulting in minimal damping of the vibrational mode and an exceptionally narrow bandwidth.

Fig. 8. Boron carbide structure (20 at.% C). The other Raman bands that have bandwidths less than  $1\text{ cm}^{-1}$  probably have their origin in similarly decoupled "strong" bonds.

The "strong" bonds in boron carbide (20 at.% carbon) are shown in Figure 8. Again, stiff bonds between icosahedral atoms and the end-atoms of the chains are isolated by less stiff intraicosahedral bonds. The  $481$  and  $534\text{ cm}^{-1}$  bands involve stiff chain-carbon-to-icosahedral-boron bonds. They are narrow compared to the bands above  $600\text{ cm}^{-1}$  that are due to icosahedral modes, but they are broad compared to the exceptionally narrow ( $<1\text{ cm}^{-1}$  FWHM) bands observed in the Raman spectra of  $\alpha$ -rhombohedral boron and boron arsenide. Distortion of the icosahedra due to carbon atoms in their polar positions tends to disorder the boron carbide lattice and broaden the  $481$  and  $534\text{ cm}^{-1}$  bands. However, decoupling of the chain-icosahedral bonds from the icosahedra and the local order of the chain structures tends to narrow them. The result is bands of intermediate width. The C-B-C bonds in the intericosahedral chains are not believed to be especially stiff. The chain-carbon-to-chain-boron distance of  $0.14\text{ nm}^{15}$  is much too short for normal covalent bonding. If one assumes a  $\text{B}^+$  (ionic) radius of  $0.03\text{ nm}^{15}$ , then  $0.11\text{ nm}$  corresponds to the radius of the carbon atom. This radius is consistent with a slightly negatively charged carbon, since neutral carbon has a radius of  $0.09\text{ nm}$ . The chain-carbon-to-chain-boron bond may be a weak ionic bond. The combination of relatively weak chain-carbon-to-chain-boron bonds and the motion of relatively massive  $\text{CB}_3$  groups is consistent with the relatively low frequency ( $481\text{ cm}^{-1}$ ) of this chain stretching mode.

## CONCLUSIONS

The Raman spectra of  $\alpha$ -rhombohedral boron and the icosahedral boron pnictides are consistent with highly ordered materials. On the other hand, the Raman spectra of the boron carbides indicate the presence of a kind of substitutional disorder, resulting from

the presence of carbon in inequivalent chain and icosahedral positions. Both the compositional and isotopic dependence of the Raman spectra support this conclusion. The frequencies and exceptionally narrow widths of certain Raman bands are explained by the decoupling of vibrational modes from the boride lattice. This decoupling occurs because of the disparities in the stiffnesses of different types of bonds. Most of the Raman bands in the spectrum of  $\alpha$ -rhombohedral boron can be assigned to  $A_{1g}$  or  $E_g$  symmetry. However, one type of mode, in addition to having an exceptionally narrow bandwidth, does not conform to the symmetry rules of the  $D_{3d}$  point group. The source of this type of mode, which may also occur in the boron pnictides, is still under investigation.

## REFERENCES

1. B. Morosin, A. W. Mullendore, D. Emin, G. A. Slack, in Boron-Rich Solids (University of New Mexico, Albuquerque, New Mexico), Proceedings of an International Conference on the Physics and Chemistry of Boron and Boron-Rich Borides, AIP Conf. Proc. No. 140, edited by D. Emin, T. L. Aselage, C. L. Beckel, I. A. Howard, and C. Wood, eds. (AIP, New York, 1986), pp. 70-86.
2. M. N. Alexander, in Boron-Rich Solids, Ref. 1, pp. 168-176.
3. G. A. Slack, T. F. McNelly, and E. A. Taft, J. Phys. Chem. Solids 44, 1009(1983).
4. M. Bouchacourt and F. Thevenot, J. Less-Common Metals 82, 219(1981).
5. C. Wood and D. Emin, in Defect Properties and Processing of High-Technology Nonmetallic Materials, Boston, 1983, Vol. 24 of Materials Research Society Symposia Proceedings, edited by J. H. Crawford, Y. Chen, and W. A. Sibley (North-Holland, Amsterdam, 1984), p. 199.
6. D. R. Tallant, T. L. Aselage, A. N. Campbell, and D. Emin, Phys. Rev B 40, 5649(1989).
7. W. Weber and M. F. Thorpe, J. Phys. Chem. Solids 36, 967(1975).
8. C. L. Beckel, University of New Mexico, private communication.
9. W. Richter, W. Weber, and K. Pfloog, J. Less-Common Met. 47, 85(1976).
10. T. C. Damen, S. P. S. Porto, and B. Tell, Phys. Rev. 142, 570(1960); Phys. Rev. 144, 771(1966).
11. D. Emin, I. A. Howard, T. A. Green, and C. L. Beckel, in Novel Refractory Semiconductors, Vol. 97 of the Materials Research Society Symposium Proceedings, edited by D. Emin, T. L. Aselage, and C. Wood (MRS, Pittsburgh, PA, 1987), pp. 83-88.
12. D. Emin, Phys. Rev. B 38, 6041(1988).
13. D. Emin, this proceedings.
14. I. Laulicht and V. Halpern, Amer. J. Phys. 39(2), 154(1971).
15. T. L. Aselage and D. Emin, this proceedings.